

Combinatorial Methods Study of Confinement Effects on the Reaction Front in Ultrathin Chemically Amplified Photoresists

Michael X. Wang, Eric K. Lin, Alamgir Karim, and Michael J. Fasolka

Polymers Division, National Institute of Standards and Technology, Gaithersburg, MD 20899

Abstract. Sub-100 nm lithography requires more understanding of photoresist material properties and processing conditions to achieve necessary critical dimension control of patterned structures. As resist thickness and feature linewidth decrease, fundamental material properties of the confined resist polymer can deviate from bulk values and impact important processing parameters such as the postexposure bake (PEB) temperature. The significance of these confinement-induced deviations on image or linewidth spread have just been reported recently by Goldfarb *et al.*. Using a high throughput combinatorial method, we explore this problem much more efficiently, and thoroughly, while offering an increased amount of data. In this work, we employed temperature and thickness gradients to characterize the spatial extent of the reaction-diffusion process in a model chemically amplified photoresist system as a function of PEB temperature and protected polymer thickness. Bilayer samples were prepared with a bottom layer of a protected polymer [poly(p-tert-butoxycarboxystyrene)] and a top layer of a deprotected polymer [poly(4-hydroxystyrene)] loaded with 5 % by mass fraction of a photoacid generator. After flood exposure, PEB, and development, changes in the thickness of the protected polymer provided a measure of the extent of the reaction front between the polymer layers. The velocity of the reaction front was significantly reduced with decreasing thickness of the protected polymer layer when its thickness was less than 60 nm or with decreasing PEB temperature under identical processing conditions.

INTRODUCTION

Sub-100 nm lithography requires a better understanding of photoresist material properties and processing conditions to achieve necessary critical dimension (CD) control of patterned structures, as well as minimal line-edge roughness (LER). Besides material properties, many processing factors can impact both CD and LER, including film thickness, exposure dose, postexposure bake (PEB) temperature, PEB time, developer concentration, and development time. For example, film thickness has a significant effect on acid reaction-diffusion rate, possibly due to a change in the local chain dynamics in thin films [1,2]. However, it is not completely understood how these variables contribute to CD and LER. In addition, due to the large number of parameters, development and optimization of resist systems or formulations is time consuming. Accordingly, integration of high throughput combinatorial research and development

strategies provides a means to effectively conduct fundamental lithographic materials research [3,4].

The diffusion of photogenerated acid (PAG) during PEB in the photoresist has been identified as a primary source of image blur and CD control [5]. In a typical positive-tone resist system, acid species generated by radiation and thermal diffusion during PEB can catalyze deprotection reaction of a large number of protection groups and make it soluble. The spatial extent of this deprotection reaction is known to be dependent on the system dimensions, i.e. film thickness and feature size. For example, it was reported that the glass transition temperature of ultrathin resist films can be dramatically different from its bulk property [6], and associated thin film confinement effects on diffusion-reaction rate were observed in a model bilayer system recently by Goldfarb *et al.* [1].

In the work of Goldfarb *et al.*, a model bilayer system consisting of a protected bottom layer and deprotected top layer loaded with a PAG was used.

The bilayer system emulates the interface between exposed and unexposed regions in a patterned photoresist. In this simplified approach, a flood exposure removes the contribution of the aerial image to the spatial distribution of acid in the resist. During PEB, the acid may diffuse into the protected layer creating an advancing front of deprotection. After development, changes in the thickness of the protected layer are used to identify the final position of the reaction boundary. By studying bilayer samples prepared under identical exposure and PEB conditions, observed changes are related to confinement-induced effects from either the substrate or the confinement itself. In this work, we follow this simple experimental scheme, but adopt high throughput methods to study PEB temperature and protected layer thickness effects by using temperature and thickness gradients, respectively.

EXPERIMENTAL

The deprotected polymer [poly(4-hydroxystyrene)] (PHS) and with number average molecular weight of 19.0 kg/mol and the fully protected polymer [poly(tert-butoxycarboxystyrene)] (PBOCSt) with number average molecular weight of 15.3 kg/mol were prepared by free radical polymerization. Di(t-butylphenyl) iodonium perfluorooctanesulfonate (PFOS) acid was obtained from DayChem. Propylene glycol methyl ether acetate (PGMEA), hexamethyldisilazane, toluene and 1-butanol were purchased from Aldrich and used without further purification. Developer CD-26 (tetramethylammonium hydroxide (TMAH) 0.26 N) was obtained from Shipley [7].

Film thickness was measured using a Filmetrics F20 UV-visible interferometer with a spot of 2 mm diameter. The n and k dependences of wavelength were determined from a thick PBOCSt film (800 nm) using a Cauchy model. The reflectivity spectrum was then fit with thickness as the only variable. The film thickness calculated with this technique was also compared to the value obtained from x-ray reflectivity. Though the thickness obtained from the interferometer was generally 2 nm larger than that from x-ray reflectivity, thickness changes should be very close from two measurements. Here, only interferometer data were used. Film thickness standard uncertainty was within ± 1 nm. Roughness was measured via atomic force microscopy (DI 3000 AFM, Digital Instruments) in tapping mode using commercial software. The scan size was $10 \mu\text{m} \times 10 \mu\text{m}$. RMS is calculated as the standard deviation of the height values within the measured area.

Samples consisted of bilayers of protected PBOCSt (bottom) and deprotected PHS (top) polymers on a hydrophobic silicon substrate. Thin $\langle 100 \rangle$ silicon wafers (Silicon, Inc.; (350 to 450) μm thick; 100 mm in diameter) were O_2 plasma cleaned to remove residual organic contaminants and treated with HF acid to remove the native silicon oxide surface. A controlled oxide layer was then regrown in a UV ozone chamber to a thickness of (10 to 20) \AA . A hydrophobic surface was generated by treating the silicon wafers with hexamethyldisilazane vapor prime in a vacuum oven.

Two approaches were used to prepare the bottom PBOCSt layer for PEB and thickness gradients. For the PEB study, the PBOCSt layer was spin cast from solution in PGMEA at 33 rad/s and subsequently baked at 100 $^\circ\text{C}$ for 60 s on a vacuum hot plate (1100 CEE, Cost Effective Equipment) after which the film thickness was measured. For the thickness confinement study, the bottom layer was prepared by a custom-made "flow coater" [8]. This device consists of a doctor blade suspended over the specimen substrate mounted on a computer controlled motion stage. A small bead of PBOCSt solution (4.8 % by mass fraction in a 50:50 mixture of PGMEA and toluene) was inserted between the blade and the substrate. Subsequently, the stage was moved at constant acceleration to spread the solution. As the solvent evaporates a thickness gradient was formed along the direction of stage motion. Here, the solvent evaporation rate was adjusted such that the solution spread well without dewetting. To achieve this, the silicon wafer was heated to 105 $^\circ\text{C}$ during the flow coating process, and toluene was added to the solution mixture. After casting, the films were kept at 90 $^\circ\text{C}$ for at least 12 h under vacuum ($< 10^{-3}$ Pa) to remove residual solvent. Then, the film thickness was measured on a 2D grid every 2 mm.

The bilayer was completed by spin casting a PHS layer onto the PBOCSt film from a 1-butanol solution with (5 % PHS by mass fraction and 5 % PFOS by mass fraction relative to the mass of PHS). The bilayer was baked at 100 $^\circ\text{C}$ for 60 s. Next, the bilayer system was exposed to a broadband UV source (Oriol Instruments) with wavelengths from 220 nm to 260 nm for a total dose of 500 mJ/cm^2 . To remove postexposure delay effects, the PEB was carried out within 5 min. The single-thickness specimen was baked on a contact hotplate with a temperature gradient ranging from 70 $^\circ\text{C}$ to 140 $^\circ\text{C}$ for 60 s; while the sample with a thickness gradient was baked at 100 $^\circ\text{C}$ on the vacuum hotplate for selected times.

After the PEB the bilayer films were developed by immersing the film in TMAH 0.26 N for 30 s, followed by a de-ionized water rinse. This removes

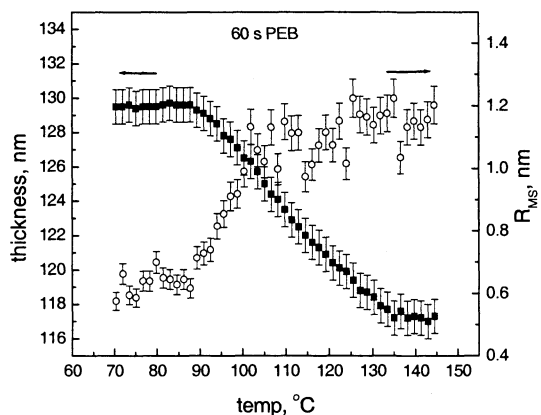


FIGURE 1. Measured thickness and roughness of remaining PBOCSt at different PEB temperatures. The error bars represent the maximum standard deviation in the measurements.

the PHS top layer and the deprotected section of the PBOCSt bottom layer. Finally, the thickness of the remaining PBOCSt layer was remeasured in 2 mm increments over a 2D grid; while the roughness was measured from areas with different thickness.

RESULTS AND DISCUSSION

Figure 1 shows the post development PBOCSt layer thickness and roughness as a function of the PEB temperature. When the PEB is below 87 °C, there are no observable changes in thickness and roughness. From 87 °C to 135 °C, the thickness decreases as PEB temperature increases, indicating that the reaction-diffusion front moves faster at the higher PEB temperature in this temperature range. The roughness (R_{SM}) increases to (1.1 ± 0.1) nm at 105 °C from (0.6 ± 0.1) nm but does not change at higher temperatures. Above 135 °C, the thickness does not change, but an apparent color change (as compared to other areas) was noted, suggesting that the possible PBOCSt decomposition has occurred, as reported by Lenhart [4]. Note here that all data were collected from the same wafer, which underwent identical procedures except the baking temperature. In addition, the data points collected in the direction vertical to the temperature gradient underwent identical processing conditions enabling significant decrease of the statistical error. Accordingly, considering the complex processing and environmental sensitivity of these

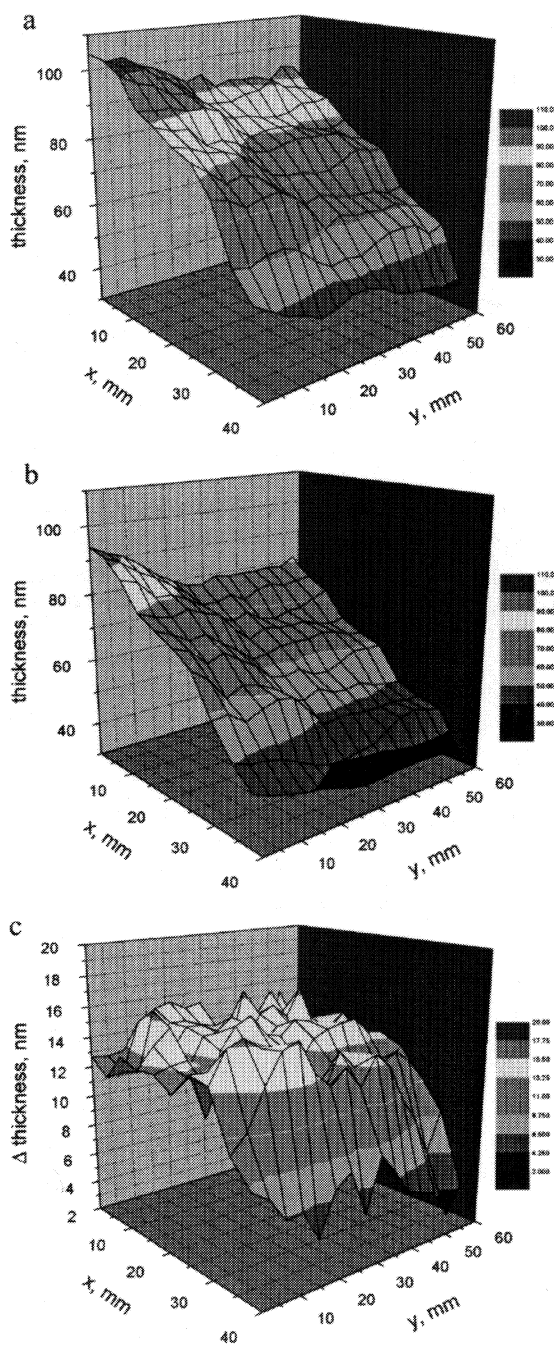


FIGURE 2. 3D plots of PBOCSt layer thickness before (a) and after (b) PEB for 60 s, and thickness change (c).

photoresist systems, this high throughput approach offers a promising method, which provides rapid and more complete results compared to traditional techniques.

Figure 2 shows representative 3D plots of PBOCSt layer thickness before (a) and after (b) the 60 s PEB and the change of thickness (c). Figure 2a shows the flow coating thin film had a thickness gradient along x direction with some variations in y direction. These defects may change the interface and consequently make the reaction-diffusion rates different from a smooth surface. We use a small step (2 mm) to map the film thickness, which masks the areas with sharp peaks and valleys. Accordingly, these films were dried completely before proceeding, since the concentration of the residual solvents depends on the local film thickness and may introduce effects besides the confinement on the reaction-diffusion rate. Figure 2c is the result of subtracting Figure 2b from Figure 2a. The plateau, where the original thickness is above (60 ± 5) nm, shows no thickness dependence. The fact that the Δd decreases with decreasing original thickness of PBOCSt layer below (60 ± 5) nm suggests that the thin film confinement has dramatically slowed down the reaction-diffusion rate.

In order to quantify the thickness effects on the reaction-diffusion rate, the final thickness changes were averaged over the points with same original film thickness (1 nm bin). The statistic error is less than 1.5 nm. Figure 3 shows thickness changes of the PBOCSt layer as a function of the PEB time for different film thickness. For all thicknesses, the Δd increases with PEB time below 60 s, while there is no difference between 60 s and 90 s. The time dependence of Δd does not exactly follow a Fickian equation as Goldfarb *et al.* reported [1]. One possible reason is that we did not maintain identical processing conditions for each wafer resulting in apparent changes in the reaction-diffusion rate. The almost equivalent Δd after 60 s and 90 s PEB times indicates that the deprotection reaction has stopped after 60 s in current processing conditions. This may be due to acid trapping or neutralization via base molecules from environment contamination. Nevertheless, because the process conditions are identical within a thickness gradient specimen, the thickness dependence of Δd shows very similar behavior for different PEB times. Indeed, this "processing consistency" is an extra advantage of using these combinatorial methods. The AFM roughness measurements for all samples gives same R_{ms} (1.2 ± 0.1) nm, showing no thin film confinement effects, indicating that the LER will be similar for all thickness.

To summarize, PEB temperature can change the acid reaction-diffusion rate significantly and have effects on surface roughness and thus LER by using a PEB temperature gradient approach. On the other hand, a strong thickness dependence of reaction-

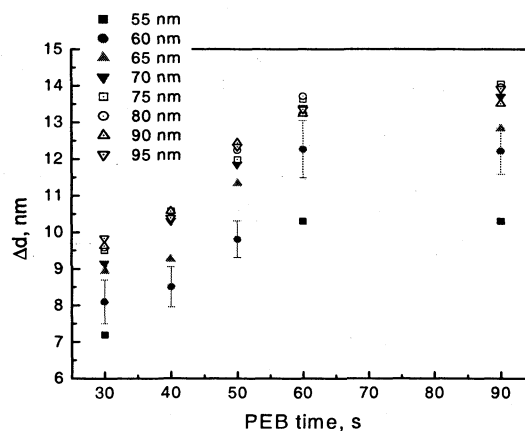


FIGURE 3. Thickness change of PBOCSt layer as a function of PEB times for different film thickness. The related standard uncertainty are similar for each data point and were only shown for 60 nm as an example.

diffusion front was confirmed by using a thickness gradient technique. The surface roughness and thus LER is independent on the thickness. An effort to combine the PEB temperature and thickness dependencies in a single specimen is currently under way. The main challenge here is to create smooth thickness gradient. In addition, we are developing means to fabricate exposure dose gradients and developer concentration gradients, which can be combined with PEB and thickness gradients for more extensive and efficient combinatorial studies of photoresist systems.

ACKNOWLEDGMENTS

This work was partially supported by the Defense Advanced Research Projects Agency Advanced Lithography Program under grant N66001-00-C-8083 as well as by the NIST Combinatorial Methods Center. We thank IBM for providing the PHS and PBOCSt materials used in this study.

REFERENCES AND NOTES

1. Goldfarb, D. L., Angelopoulos, M., Lin, E. K., Jones, R. L., Soles, C. L., Lenhart, J. L., and Wu, W., *J. Vac. Sci. Technol.* **B19**, 2699-2704 (2001).

2. Soles, C. L., Douglas, J. F., Lin, E. K., Lenhart, J. L., Jones, R. L., Wu, W., Goldfarb, D. L. and Angelopoulos, M., *J. Appl. Phys.*, **93**, 1978-1986 (2003).
3. Meredith, J. C., Smith, A. P., Karim, A., and Amis, E. J., *Macromolecules* **33**, 9747-9756 (2000).
4. Lenhart, J. L., Jones, R. L., Lin, E. K. Soles, C. L., Wu, W., Goldfarb, D. L., and Angelopoulos, M., *J. Vac. Sci. Technol.* **B20**, 704-709 (2002).
5. Houle, F. A., Hinsberg, W. D., Morrison, M., Sanchez, M. I., Wallraff, G., Larson, C., and Hoffnagle, J., *J. Vac. Sci. Technol.* **B18**, 1874-1885 (2000).
6. Fryer, D. S. Nealey, P. F., and de. Pablo, J., *Macromolecules* **33**, 6439-6447 (2000).
7. Commercial equipment and materials are identified in this proceeding only to adequately specify experimental procedure. In no case does this imply endorsement or recommendation by the National Institute of Standards and Technology.
8. Meredith, J. C., Karim, A., and Amis, E. J., *Macromolecules* **33**, 5760-5762 (2000).